Published in final edited form as:
Cancer Res. 2012 February 15; 72(4): 897–907. doi:10.1158/0008-5472.CAN-11-2681.

Hedgehog signaling inhibition blocks growth of resistant tumors through effects on tumor microenvironment

Emanuela Heller[1,*], **Michelle A. Hurchla**[1,*], **Jingyu Xiang**[1], **Sara Chen**[1], **Jochen Schneider**[2], **Kyu-Sang Joeng**[3], **Marcos Vidal**[4], **Leah Goldberg**[1], **Hongju Deng**[1], **Mary C. Hornick**[1], **Julie L. Prior**[5], **David Piwnica-Worms**[5], **Fanxin Long**[3], **Ross Cagan**[6], and **Katherine N. Weilbaecher**[1]

[1]Department of Medicine, Division of Oncology, Washington University School of Medicine, St. Louis, MO, USA

[2]Luxembourg Centre for Systems Biomedicine, University of Luxembourg, Luxembourg

[3]Department of Medicine, Division of Endocrinology, Metabolism and Lipid Research, Washington University School of Medicine, St. Louis, MO, USA

[4]The Beatson Institute for Cancer Research, Glasgow, UK

[5]BRIGHT Institute and Molecular Imaging Center, Mallinkrodt Institute of Radiology, Washington University School of Medicine, St. Louis, MO, USA

[6]Department of Developmental and Regenerative Biology, Mount Sinai School of Medicine, New York, NY

Abstract

Hedgehog (Hh) signaling is implicated in bone development and cellular transformation. Here we demonstrate that inhibition of Hh pathway activity inhibits tumor growth through effects on the microenvironment. Pharmacological inhibition of the Hh effector *Smoothened* (*Smo*) increased trabecular bone in vivo and inhibited osteoclastogenesis in vitro. In addition, enhanced Hh signaling due to heterozygosity of the Hh inhibitory receptor *Patched* (*Ptch1*+/−) increased bone resorption, suggesting direct regulation of osteoclast activity by the Hh pathway. *Ptch1*+/− mice had increased bone metastatic and subcutaneous tumor growth, suggesting that increased Hh activation in host cells promoted tumor growth. Subcutaneous growth of Hh-resistant tumor cells was inhibited by LDE225, a novel orally bioavailable Smo antagonist, consistent with effects on tumor microenvironment. Knockdown of the Hh ligand Sonic Hh (*SHH*) in these cells decreased subcutaneous tumor growth and decreased stromal cell production of IL-6, indicating that tumor-derived Hh ligands stimulated tumor growth in a paracrine fashion. Together our findings demonstrate that inhibition of the Hh pathway can reduce tumor burden, regardless of tumor Hh responsiveness, through effects on tumor cells, osteoclasts and stromal cells within the tumor microenvironment. Hh may be a promising therapeutic target for solid cancers and bone metastases.

Keywords

hedgehog; osteoclast; cyclopamine; LDE225; tumor microenvironment

Corresponding author: Katherine Weilbaecher, Department of Medicine, Division of Oncology, Washington University School of Medicine, 660 S. Euclid Ave, Box 8069, St. Louis, MO, 63110, USA kweilbae@dom.wustl.edu.
*authors contributed equally

Introduction

The Hedgehog (Hh) signaling pathway plays critical roles in epithelial-mesenchymal transition and cell differentiation during embryonic development (1, 2), adult tissue homeostasis and tumorigenesis (3, 4). In the absence of ligand, the Hh receptor Patched (Ptch) inhibits the activator Smoothened (Smo). Upon ligand binding to Ptch, Smo is released, resulting in pathway activation and transcription of target genes including *Gli1, Gli2* and *Ptch1* (5, 6). Cyclopamine, a naturally occurring Hh inhibitor and Smo antagonist, first highlighted the importance of Hh signaling. Several next-generation analogues with increased specificity and tolerability (7) (including GDC-0449, LDE225 and IPI-926) exert anti-tumor effects in a subset of cancer cells and are currently in clinical trials for a wide variety of tumors (8-10).

The Hh signaling pathway plays a critical role in tumorigenesis and progression in many tumor types. Mutations leading to ligand-independent Hh pathway activation have been linked to basal cell carcinoma and medulloblastoma (11, 12) while overexpression of the Hh ligand Sonic hedgehog (*Shh*) or mutations in Hh signaling genes (*Smo, Ptch1, Gli1, Gli2*) have been implicated in the emergence and progression of numerous epithelial cancers including breast, skin, esophagus, stomach, pancreas, liver, lung and prostate (11, 13, 14). Hh inhibition via cyclopamine suppressed proliferation of breast carcinoma cell lines and decreased *Gli1* (15, 16). These effects are not limited to primary tumors, as inhibition of the Hh pathway decreased lung and liver metastases in a mouse pancreatic cancer model together with gemcitabine (17, 18).

In addition to direct effects on tumor cell growth, Hh signaling within the host stromal microenvironment also controls tumor progression. Mice with a targeted disruption of the Hh inhibitory receptor *Ptch1* develop ductal hyperplasia (15). Interestingly, it was disruption of *Ptch1* in mammary stroma rather than in mammary epithelium that led to the ductal changes, suggesting an indirect effect of Hh signaling on tumor-initiating cells. Furthermore, paracrine Hh activation in host-derived stromal cells leads to increased tumor growth (19-21) and is necessary to support the growth of stromal-dependent B cell lymphoma and multiple myeloma (22). Increased intra-tumoral expression of Hh target gene *Gli2* increased production of osteoclast (OC) activating factor PTHrP in breast cancer cells, linking Hh signaling with tumor-induced osteolysis (23). However, in certain breast cancer cell lines that are relatively resistant to Hh signaling modulation, *Gli2* expression can be induced through TGFβ signaling independent of Hh resulting in enhanced osteolysis (24). Together these studies provide a strong rationale for evaluating Hh signaling as a therapeutic target for cancer and metastasis.

The Hh pathway is critical to osteoblast (OB) differentiation and chondrocyte proliferation during embryonic endochondral bone development (25, 26). Targeted disruption of several Hh pathway genes result in profound effects on bone development (27-29). Postnatal interruption of the Hh pathway leads to trabecular bone abnormalities and disrupted long bone formation (30, 31). The effects of Hh signaling interruption on adult bone have not been fully elucidated. Mice with conditional deletion of *Ptch1* in mature OB using osteocalcin-Cre show increased production of RANK ligand (RANKL) by OB which indirectly increased OC activity and bone loss (32). However, mice with heterozygous germline deletion of *Ptch1* (*Ptch1*+/−) show increased bone mass, with enhanced bone formation being dominant to increased in vivo OC number and resorption (33). The discrepancy between the two models remains to be fully resolved. Interestingly, direct effects of Hh pathway signaling on OC have not been reported.

We hypothesized that disruption of Hh signaling would block tumor growth both directly by targeting intratumoral survival signaling and indirectly by altering the host microenvironment. Indeed, OC and OB-derived proteins such as TGFβ can enhance growth of bone-invading tumor cells (34), and we propose that the effects of Hh signaling in both tumor and host cells may enhance metastatic growth. In this study we demonstrate that disruption of the Hh pathway in adult non-tumor bearing mice increased trabecular bone in part through reduced OC function and identified a cell-autonomous role of Hh signaling during osteoclastogenesis. Employing pharmacologic inhibitors, we show that disruption of the Hh pathway decreased subcutaneous and bone tumor burden *in vivo*. Mice heterozygous for Ptch, resulting in systemically enhanced Hh signaling, also had increased tumor burden. Moreover, Hh inhibitors decreased subcutaneous tumor burden in a cell line that is resistant to direct cytotoxic effects due to reduced Smo expression (24), demonstrating indirect anti-tumor effects of targeting cells of the host microenvironment. Interestingly, MDA-MB-231 cells produce Hh ligands and knockdown of SHH decreased tumor growth through paracrine effects on stromal cell production of growth factors including IL-6. Thus, Hh inhibitors represent promising therapeutics due to their ability to target both tumor cells and the pro-tumor microenvironment.

Materials and Methods

Animals

Female BALB/c mice and athymic nude mice (NCr-nude) were obtained from Taconic (Hudson, NY). *Ptch*+/− (12) and *Smo*$^{fl/fl}$ (25) mice on C57Bl/6 and mixed backgrounds respectively, were previously described. Animals were housed under pathogen-free conditions according to the guidelines of the Division of Comparative Medicine, Washington University. The animal ethics committee approved all experiments.

Cells

4T1 BALB/c murine breast cancer (35) and B16-F10 C57Bl/6 murine melanoma cell lines (36) were purchased from the American Type Culture Collection and modified to express firefly luciferase as previously described. A bone metastatic variant of MDA-MB-231, described in (37), was a kind gift of T. Guise (Indiana University). Low passage stocks were utilized and regularly tested for mycoplasma and maintenance of growth characteristics.

Drug compounds and dosing

The following drugs were used as indicated: cyclopamine (LC Labs, Woburn, MA), tomatidine (Sigma, St. Louis, MO), GDC-0449 (provided by Dr. Jim Janetka, Washington University), and LDE225 (provided by Novartis Pharmaceuticals). Cyclopamine (25mg/kg) was administer per oral gavage twice daily for 11-14 days as previously described (17); LDE225 (20mg/kg) once daily for 21 days orally.

Micro–computed tomography

Post-mortem, tibiae and femurs were scanned (μCT-40; Scanco Medical) and evaluated as described previously (36).

Bone histology and *in vitro* OC quantification

Decalcified and paraffin embedded sections were stained with H&E or TRAP. Images were taken with an Eclipse TE300 inverted microscope (Nikon, Tokyo, Japan) using the 4x (H&E, TRAP, in vitro OC) or 40x (actin rings, pits) objectives. Histomorphometry was performed using BioQuant Osteo (Nashville, TN).

Serum CTX and osteocalcin

Serum from overnight fasted mice was measured by ELISA for CTX (RatLaps, Immunodiagnostic Systems, Scottsdale, AZ) and osteocalcin (Biomedical Technologies Inc, Stoughton, MA) according to the manufacturer's instructions.

Macrophage and OC generation

To generate macrophages, whole bone marrow cells were cultured in αMEM with 10% FBS and 100 ng/ml M-CSF for 3 days. To generate OCs, macrophages were cultured in αMEM, 10% FBS, 50 ng/ml M-CSF and 50 ng/mL RANKL for 6 days (36, 38). Media was refreshed every 2 days. Cells were fixed and stained for tartrate-resistant acid phosphatase (TRAP) using the leukocyte acid phosphatase kit (Sigma).

Lentiviral production and infection

293T cells were transfected with plasmid of interest, pHR'8.2deltaR and pCMV-VSV-G using Xtreme Gene 9 (Roche, Indianapolis, IN) and supernatant harvested 48 hours later. Cells were infected with lentivirus-containing supernatant for 4 hours in the presence of 10 μg/ml protamine sulfate. For ex vivo *Smo* excision, $Smo^{fl/fl}$ macrophages were infected with virus produced from pHR'EF-Cre-WPRE-SIN ('CRE') or pHR'EF-GFP-WPRE-SIN ('GFP') virus in the presence of 50ng/ml M-CSF. 48 hours after infection, macrophages were screened for excision efficiency and differentiated into OC. For *SHH* knockdown, shRNA constructs in pLKOpuro vectors were obtained from the Washington University Genome Institute and Children's Discovery Institute RNAi Consortium. (shLacZ–CGCGATCGTAATCACCCGAGT; shSHH-2– GCTGATGACTCAGAGGTGTAA; shSHH-3– CATATCCACTGCTCGGTGAAA). Transduced cells were selected with 2 μg/ml puromycin.

Quantitative reverse transcription PCR (qRT-PCR)

RNA was extracted using RNeasy Mini kit (Qiagen, Valencia, CA), treated with DNaseI and reverse transcribed using iScript (Bio-Rad, Hercules, CA). A no-RT control was included in each assay.Quantitative PCR was performed using SsoFast EVA Green Supermix (Bio-Rad). Experiments were performed in duplicate for both the target and the endogenous gene (GAPDH for OC, cyclophilin for BMSC and MDA-MB-231) used for normalization. Relative quantification of the target gene expression was calculated by the comparative threshold cycle (Ct) method: $2^{-\Delta\Delta Ct}$ where ΔCt = Cttarget gene–Ctendogenous gene and ΔΔCt=ΔCtvehicle–ΔCttreated. See supplemental methods for primer sequences.

Actin ring and bone resorption assay

3,000 day 3 pre-osteoclasts differentiated as above were plated on bovine bone slices in 96 well plates. At day 6, actin rings and resorption lacunae were visualized as previously described (36).

BrdU proliferation assay

2.5×10^4 cells/mL were plated with indicated drug concentrations. Cells were labeled with BrdU for 24 hours and processed according to the manufacturer's instructions (Cell Proliferation ELISA, Roche).

Immunoblotting

50 μg protein was separated on 8% SDS-polyacrylamide gels and transferred onto a PVDF membrane and incubated with p-AKT-Substrate, p-ERK, or total-ERK rabbit antibodies (Cell Signaling Technology, Danvers, MA), followed by horseradish peroxidase-conjugated

anti-rabbit secondary antibody (Amersham Bioscience, Piscataway, NJ). Specific bands were developed by enhanced chemiluminescence. Loading control was β-actin (clone AC15; Sigma).

Tumor models

Intra-cardiac (1×10^5 cells) and intra-tibial (1×10^4 cells) tumor cell injections were performed as previously described (36). For subcutaneous injections 1×10^6 (4T1 and B16) or 2×10^6 (MDA-MB-231) tumor cells were injected in a 1:1 ratio with Matrigel (BD Biosciences) as previously described (36, 38).

In vivo bioluminescence imaging (BLI)

Imaging was performed on a IVIS 100 device (Caliper Life Sciences, Hopkinton, MA) as previously described (36), except that for subcutaneous tumor image analysis, a software-defined contour region of interest (ROI) was used to measure total photon flux.

MTT viability assay

5,000 cells/well were plated in 96 well plates with indicated concentrations of drug. After 48 hours, 10μL MTT (Sigma) was added for 4 hours. HCl/isopropanol was added to measure absorbance at 570nm and 630nm.

Bone marrow chimeras

Recipient mice were lethally irradiated (1000 rads). 24 hours later, 1×10^6 donor whole bone marrow cells were transferred intravenously into recipient mice. After 4 weeks, hematopoietic reconstitution with the donor genotype was confirmed by PCR of peripheral blood and mice were challenged with the B16 tumor.

Bone marrow stromal cell (BMSC) culture

To generate BMSC, whole bone marrow of WT C57BL/6 mice was cultured in αMEM with 20% FBS for 7 days and adherent cells replated at 5×10^5 cells/ml. At confluence, recombinant murine Shh (Ebioscience, San Diego, CA) or a 50:50 dilution of tumor cell conditioned media (from 3×10^6 cells, 24 hours in serum-free media) was added and cultured for an additional 72 hours in αMEM with 2.5% FBS.

Statistical analysis

Experiments were analyzed using two-tailed Student's *t*-test or ANOVA using Prism5 (Graphpad, LaJolla, CA). Errors bars represent SEM. Results were considered to reach significance at $p\leq0.05$ and are indicated with an asterisk (*).

Results

Cyclopamine increased bone mass and suppressed OC function in non-tumor bearing mice

To understand the effect of Hh signaling on adult non-tumor bearing bone, we administered the Hh inhibitor cyclopamine to adult mice by twice daily by oral gavage for 14 days and observed increased trabecular bone volume and thickness (Fig. 1A-D). Despite a non-significant increase in OC number (Fig. 1E), serum CTX, a marker of osteoclastic bone resorption, was significantly decreased with cyclopamine (Fig. 1F). Serum osteocalcin, a marker of osteoblast activity, showed a non-significant reduction after Hh inhibition (Fig. 1G). Thus, pharmacologic inhibition of Hh signaling led to increased trabecular bone mass, with evidence of decreased OC function *in vivo*.

Disruption of Hedgehog signaling inhibited ex vivo osteoclastogenesis in a cell-autonomous manner

To test whether Hh signaling had direct effects on OC formation, we disrupted *Smoothened* by transducing $Smo^{fl/fl}$ bone marrow macrophages (BMMs) with a lentivirus expressing Cre-recombinase (Fig. S1A) and subjected the cells to osteoclastogenesis. We observed a decrease in OC size and number after *Smo* excision compared to GFP transduced control cells (Fig. 2A-B). Furthermore, pharmacological inhibition of Smo with cyclopamine (Fig. S1B) or LDE225 (Fig. 2C) resulted in a dose-dependent decrease in TRAP+ multinucleated OC formation. Likewise, LDE225 reduced the mRNA abundance of the Hh target *Gli1* and of the OC differentiation markers NFATc1 (*Nfatc1)*, β3 integrin (*Itgb3*), and cathepsin K (*Ctsk*) (Fig. 2D). Furthermore, treatment of preOCs with recombinant murine Shh increased mRNA transcripts of *Gli1*, *Nfatc1*, and *Itgb3*, suggesting that Hh stimulation enhanced signaling pathways involved in OC differentiation (Fig. 2E). These results suggest that Hh signaling through *Smo* is critical to normal OC formation in a cell-autonomous fashion.

Enhanced Hh signaling due to *Ptch1*-heterozygosity increased OC function in a cell-autonomous manner

Adult *Ptch1*+/− with enhanced Hh signaling, had elevated serum CTX, indicating increased bone resorption (Fig. 3A). Interestingly, subjecting equal numbers of WT and *Ptch1*+/− BMMs to osteoclastogenesis, *Ptch1*+/− OC formed increased actin rings and resorption lacunae when plated on bone (Fig. 3B-C), but showed no difference in osteoclastogenesis on plastic (Fig. S2A). We observed increased proliferation of *Ptch1*+/− BMMs (Fig. 3D) and increased levels of phospho-AKT substrates (p-AKTs) in day 3 *Ptch1*+/− pre-OC (Fig. 3E). However, we did not observe a difference in the expression of phosphorylated ERK in BMMs (Fig. S2B) nor in rate of apoptosis of *Ptch1*+/− OCs (Fig. S2C). From these data we conclude that enhanced Hh signaling promoted macrophage proliferation and OC function.

Hedgehog pathway inhibition with cyclopamine decreased bone metastases in a murine breast cancer model

To test whether Hh inhibition would reduce bone tumor burden, we challenged immunocompetent BALB/c mice with osteolytic murine 4T1 mammary breast carcinoma cells (35). Cyclopamine significantly decreased tumor burden in bone after either intra-cardiac (Fig. 4A-D) or intra-tibial (Fig. 4E) injection. These data demonstrate that Hh antagonism decreased bone metastatic tumor growth in immunocompetent mice.

Smo antagonists exert direct cytotoxic effects on 4T1 breast cancer cells

In vitro analyses demonstrate that 4T1 tumor cells have intact Hh signaling pathways that are responsive to Smo antagonism. Cyclopamine decreased the viability and proliferation of 4T1 cells in a dose-dependent manner (Fig. 5 A-B). mRNA expression of the downstream target *Gli1* was also significantly decreased with cyclopamine (Fig. 5C). The small molecule Smo inhibitor GDC-0449 (Fig. S3A) also decreased 4T1 viability, while tomatidine, an inactive structural analog of cyclopamine, had no effect (Fig. S3B). Compared to vehicle controls, subcutaneous growth of 4T1 cells in Balb/c mice was significantly reduced by cyclopamine (Fig. 5D). These data are consistent with a direct inhibition of tumor growth, however the specific contribution of host-targeted Smo antagonism cannot be evaluated in this model.

Enhanced Hh signaling due to *Ptch1*-heterozygosity indirectly enhanced tumor growth

To examine the possibility that Hh signaling may play a role in various tissues through mechanisms independent of direct anti-tumor actions, we evaluated tumor growth in *Ptch1*+/− mice. Following intra-cardiac injection of osteolytic B16 cells into immunocompetent

C57Bl/6 mice, metastatic bone tumor burden was significantly increased in *Ptch1*+/− mice compared to WT littermates (Fig. 6A-D). We also observed an increase in subcutaneous B16 tumor burden in *Ptch1*+/− mice (Fig. 6E), suggesting that the tumor-promoting effects of enhanced Hh signaling in the host are not specific to the bone environment. To test whether this was due to cells of hematopoietic origin (including myeloid and immune cells), we established radiation chimeras of WT and *Ptch1*+/− recipient mice reconstituted with reciprocal WT or *Ptch1*+/− bone marrow. In both WT and Ptch1+/− recipients, reconstitution with *Ptch1*+/− hematopoietic cells increased B16 subcutaneous tumor growth compared to reconstitution with WT bone marrow (Fig. 6F-G). Flow-cytometry showed no significant differences in the extent of hematopoietic reconstitution (Fig. S4A-C). These data suggest that host Hh signaling, in part through hematopoietic cells, influenced tumor growth indirectly through the microenvironment, independent of direct effects on tumor cells.

MDA-MD-231 breast cancer cells are resistant to direct cytotoxic effects of Smo antagonists

MDA-MB-231 human breast cancer cells are reported to have non-detectable levels of *Smo* transcripts and to be resistant to killing by Smo antagonists (7, 39). In agreement, we did not observe significantly decreased viability even at micromolar concentrations of LDE225 (Fig. 7A). Reports of cytotoxicity in sensitive tumor cell lines are in the nanomolar range (40), thus demonstrating relative resistance of this tumor to in vitro cytotoxic effects. Furthermore, LDE225 treatment did not decrease the expression of Hh target genes *PTCH1* or *GLI2* in MDA-MB-231 cells (Figs. S5A-B). These data suggest that MDA-MB-231 cells are resistant to direct effects of pharmacologic Hh inhibition, allowing for a system in which to examine the microenvironment-targeted effects of Smo antagonists.

Hh signaling in host microenvironment cells influence tumor growth in vivo

To evaluate the roles of Hh inhibition directly on cells present in the tumor microenvironment, subcutaneous growth of MDA-MB-231 Hh inhibition ‘resistant’ tumor cell lines was evaluated. While the decreased growth of Hh inhibition ‘sensitive’ 4T1 cells could be attributed to direct cytotoxic effects on the tumor cells (Figs. 4-5), effects of Smo antagonists on growth of ‘resistant’ MDA-MB-231 tumors would be specifically due to modulation of the host microenvironment. In nude mice, subcutaneous growth of MDA-MB-231 cells was significantly reduced by LDE225 (Figure 7B), demonstrating that Hh inhibition isolated to host cells can modulate tumor growth.

Tumor-derived Sonic hedgehog increased tumor growth through effects on the microenvironment

Although MDA-MB-231 cells are unresponsive to canonical Hh pathway stimulation, their production of Hh ligands, particularly SHH (Fig. 7C), could stimulate Hh signaling in surrounding tissues in a paracrine fashion. To investigate the effects that tumor-produced Hh ligands have on the microenvironment, SHH expression was decreased in MDA-MB-231 cells by approximately 70% using two lentivirally-expressed shRNAs (Fig. 7D). Following knockdown, cells maintained in vitro proliferation rates similar to parental cells (Fig. S5C). In vivo, MDA-shSHH-2 and MDA-shSHH-3 formed significantly smaller subcutaneous tumors than parental or control MDA-shLacZ tumors, demonstrating that tumoral production of Hh ligands can increase growth of tumors that fail to respond to canonical Hh stimulation in an autocrine signaling (Fig. 7E).

Stromal cells within the microenvironment produce a variety of tumor-supporting growth factors. To evaluate the effects of tumor-derived SHH on stromal cells, we added conditioned media (CM) from parental MDA or MDA-shLacZ cells to murine bone marrow stromal cells (BMSC) and found that increased transcription of *Gli1* to similar levels as

recombinant Shh (Fig. S5D). In contrast, CM from MDA-shSHH-2 or MDA-shSHH-3 failed to induce BMSC *Gli1*, suggesting that Hh signaling was blunted. BMSC production of IL-6, a pro-tumor and pro-osteoclastogenic factor, was increased by recombinant Shh (Fig. 7F). CM from parental MDA or MDA-shLacZ further induced IL-6 transcription (Fig. 7F) and secretion (Fig. S5E) in BMSC, while that of MDA-shSHH-2 or MDA-shSHH-3 cells induced it to a lower extent. While tumor cells produce an abundance of factors that affect numerous stromal cells signaling pathways, this data suggests that BMSC production of IL-6 is due in part to stimulation of the Hh pathway. These data suggest that Hh inhibition in host microenvironment cells can reduce tumor burden indirectly even when tumor cells themselves are resistant to direct Hh inhibition.

Discussion

While the majority of current pharmaceuticals used in the treatment of cancer directly target tumor cell growth and survival, a growing body of evidence has demonstrated that many components of the host microenvironment are critical to tumorigenesis and represent additional therapeutic targets. Thus, therapeutic manipulation of this pathway has the potential to decrease tumor growth both through direct and indirect mechanisms. Intratumoral Hh pathway signaling has been shown to be vital for the growth and maintenance of many tumor types (3, 4). However, a number of tumors have been shown to be refractory to the direct effects of pharmacologic Hh inhibition with Smo antagonists due to natural or acquired mutations in *Smo* (24, 41) or amplification of downstream effector *Gli2* (40, 42).

Previous reports have shown that tumor growth was blunted when paracrine Hh signaling was inhibited in stromal components of the microenvironment even when the tumor itself is Smo-independent (19, 22, 43). The Hh inhibitor GDC-0449 induced dramatic reductions in the growth of tumors with activating Hh mutations (44, 45). Interestingly, GDC-0449 has little direct effect on tumors without Hh mutations; however, it significantly blocked Hh signaling in tumor stroma and decreased tumor burden (46). In this report, we found that the Smo antagonist LDE225 had potent in vivo anti-tumor activity in MDA-MB-231, an aggressive breast tumor cell line relatively resistant to Hh pathway modulation due to undetectable levels of *Smo* (7, 39). Furthermore, we demonstrate that tumoral production of the Hh ligand SHH supported growth of subcutaneous tumors in vivo. We provide evidence that this effect is due to paracrine stimulation of the Hh signaling pathway in stromal cells, resulting in the increased production of growth factors, including, but not limited to, IL-6. We also show that enhanced Hh signaling in the host environment of *Ptch1*+/− mice promoted growth of bone metastases and subcutaneous tumors, in part through contributions of hematopoietically-derived cells, including but not limited to, immune cells and OC. While the mechanisms underlying the described phenotypes still need to be further elucidated, these data underscore a role for Hh inhibition in cells of the microenvironment, even in Hh unresponsive tumor cells, and highlights the potential for increased clinical utility of Hh inhibition in cancer treatment.

In addition to its role in tumorigenesis, Hh signaling is crucial to proper development and maintenance of many host tissues including bone (25, 26). However, studies into the role of Hh signaling in post-natal bone have yielded disparate results. Enhancing Hh signaling through germline *Ptch1*-heterozygosity resulted in increased bone density (33), while conditional homozygous deletion of *Ptch1* in mature OB decreased bone density (32). Both groups observed increases in bone formation and resorption, however the effects of Hh signaling on the OC were attributed to be indirect via increased OB expression of RANKL. Here we report a previously unrecognized cell-autonomous role for Hh signaling in the differentiation of bone-resorbing OCs. We found that genetic and pharmacological Hh

inhibition decreased OC differentiation *in vitro*. Furthermore, transcription of target gene *Gli1* and key genes involved in OC differentiation (*Nfatc1, Itgb3*, and *Ctsk*) were reduced with Hh inhibition. These results are in agreement with a recent report demonstrating that RAW cell differentiation into OCs could be inhibited with cyclopamine (47). *Ptch1*+/− mice, where Hh signaling is enhanced, are known to have increased bone mineral density and OB activity (33). Concurrently, we observed that *Ptch1*+/− mice also had enhanced OC activity *in vitro*. Together these data suggest a direct, cell-autonomous role for Hh signaling in the OC.

We report that systemic Hh inhibition with cyclopamine increased bone density of adult WT mice, while a previous study found decreased bone density (33). Several differences between treatment protocols (i.e. administration and dosing), and importantly, recognized gender differences in bone biology, may explain these seemingly paradoxical results. The previous study dosed male mice with 10mg/kg cyclopamine intraperitoneally once a day (33) while we used 25mg/kg orally twice daily in females. Twice daily administration and/or increased drug dosage could result in more continuous or potent inhibition of Hh and OC function, leading to increased bone density. Similarly, continuous administration of parathyroid hormone (PTH) has catabolic effects on bone while intermittent dosing is anabolic (48). Hh signaling in bone homeostasis seems tightly regulated by the strength of signaling, as suggested in discrepant results between heterozygous (33) and homozygous loss of *Ptch1* (32). Overall our results and those of others (32, 33) suggest that level and regulation of Hh signaling in the bone microenvironment is important to properly regulate the extent of bone formation and resorption occurring under non-pathologic conditions.

As OC and tumor cells are both known to produce growth factors that support the activity of the other, the bone microenvironment is a hotspot of tumor metastasis, known as “the vicious cycle” (34). Thus, blunting tumor-driven manipulation of bone remodeling and turnover can indirectly decrease the expansion of tumor in bone. Here we demonstrate that mice treated with cyclopamine had decreased tumor burden in bone. However, as subcutaneous tumor growth was also decreased, the anti-tumor activity of Smo antagonists was due at least partially to non-bone cell effects, including those directly on tumor cells and on host stromal cells.

In conclusion, our data demonstrate that components of the Hh signaling pathway are promising therapeutic targets for cancer as they have the ability to decrease tumor growth both by exerting direct anti-tumor effects and by making the host microenvironment less hospitable to tumors. Hh inhibition has now been shown to act on a variety of host microenvironment cells, including stroma, hematopoietic cells and vasculature (49, 50) to contribute to the overall therapeutic effect. In addition to these effects on solid tumors, targeting the Hh pathway is a particularly attractive target for the treatment of bone metastases as it may prove beneficial in interrupting the vicious cycle of OB, OC and tumor cells and effectively decrease both tumor burden and tumor-associated osteolysis, which are linked to high rates of mortality and morbidity. As several small-molecule Hh signaling inhibitors are currently being clinically evaluated for efficacy in a variety of tumor types, their effect on Hh signaling in cells of the tumor microenvironment warrants active investigation.

Supplementary Material

Refer to Web version on PubMed Central for supplementary material.

Acknowledgments

We thank Steven Teitelbaum, F. Patrick Ross, Xinming Su, Deborah Novack and Roberta Faccio for helpful discussions; Ozge Uluckan, Crystal Winkeler, Ceren Yalaz, Desiree Floyd, Aixiao Li, Jean Chappel, Wei Zou, Lorena Salavaggione, Mark Wilkins, Emira Pazzoli and Georg Feldmann for technical assistance; Jim Janetka for GDC-0449 synthesis; and Crystal Idleburg for expert histology.

Grant Support: This research was supported by grants from The Department of Defense (W81XWH-07-1-036-KNW, RC), The St. Louis Men's Group Against Cancer (KNW), and the National Institutes of Health (CA097250, CA100730-KNW; T32CA113275-MAH; DK065789-FL; P50CA94056-DPW). MicroCT and histology services were provided by the WU musculoskeletal core (P30AR057235).

References

1. McMahon AP, Ingham PW, Tabin CJ. Developmental roles and clinical significance of hedgehog signaling. Curr Top Dev Biol. 2003; 53:1–114. [PubMed: 12509125]
2. Echelard Y, Epstein DJ. Sonic hedgehog, a member of a family of putative signaling molecules, is implicated in the regulation of CNS polarity. Cell. 1993; 75:1417–30. [PubMed: 7916661]
3. Jiang J, Hui CC. Hedgehog signaling in development and cancer. Dev Cell. 2008; 15:801–12. [PubMed: 19081070]
4. Taipale J, Beachy PA. The Hedgehog and Wnt signalling pathways in cancer. Nature. 2001; 411:349–54. [PubMed: 11357142]
5. Varjosalo M, Taipale J. Hedgehog signaling. J Cell Sci. 2007; 120:3–6. [PubMed: 17182898]
6. Rohatgi R, Scott MP. Patching the gaps in Hedgehog signalling. Nat Cell Biol. 2007; 9:1005–9. [PubMed: 17762891]
7. Zhang X, Harrington N, Moraes RC, Wu MF, Hilsenbeck SG, Lewis MT. Cyclopamine inhibition of human breast cancer cell growth independent of Smoothened (Smo). Breast Cancer Res Treat. 2009; 115:505–21. [PubMed: 18563554]
8. Tremblay MR, Lescarbeau A, Grogan MJ, Tan E, Lin G, Austad BC, et al. Discovery of a potent and orally active hedgehog pathway antagonist (IPI-926). J Med Chem. 2009; 52:4400–18. [PubMed: 19522463]
9. De Smaele E, Ferretti E, Gulino A. Vismodegib, a small-molecule inhibitor of the hedgehog pathway for the treatment of advanced cancers. Curr Opin Investig Drugs. 2010; 11:707–18.
10. Tremblay MR, McGovern K, Read MA, Castro AC. New developments in the discovery of small molecule Hedgehog pathway antagonists. Curr Opin Chem Biol. 2010; 14:428–35. [PubMed: 20399136]
11. Oro AE, Higgins KM, Hu Z, Bonifas JM, Epstein EH Jr. Scott MP. Basal cell carcinomas in mice overexpressing sonic hedgehog. Science. 1997; 276:817–21. [PubMed: 9115210]
12. Romer JT, Kimura H, Magdaleno S, Sasai K, Fuller C, Baines H, et al. Suppression of the Shh pathway using a small molecule inhibitor eliminates medulloblastoma in Ptc1(+/−)p53(−/−) mice. Cancer Cell. 2004; 6:229–40. [PubMed: 15380514]
13. Ribeiro-Silva A, Ramalho LN, Garcia SB, Brandao DF, Chahud F, Zucoloto S. p63 correlates with both BRCA1 and cytokeratin 5 in invasive breast carcinomas: further evidence for the pathogenesis of the basal phenotype of breast cancer. Histopathology. 2005; 47:458–66. [PubMed: 16241993]
14. Al-Hajj M, Wicha MS, Benito-Hernandez A, Morrison SJ, Clarke MF. Prospective identification of tumorigenic breast cancer cells. Proc Natl Acad Sci U S A. 2003; 100:3983–8. [PubMed: 12629218]
15. Kubo M, Nakamura M, Tasaki A, Yamanaka N, Nakashima H, Nomura M, et al. Hedgehog signaling pathway is a new therapeutic target for patients with breast cancer. Cancer Res. 2004; 64:6071–4. [PubMed: 15342389]
16. Kameda C, Tanaka H, Yamasaki A, Nakamura M, Koga K, Sato N, et al. The Hedgehog pathway is a possible therapeutic target for patients with estrogen receptor-negative breast cancer. Anticancer Res. 2009; 29:871–9. [PubMed: 19414322]

17. Feldmann G, Dhara S, Fendrich V, Bedja D, Beaty R, Mullendore M, et al. Blockade of hedgehog signaling inhibits pancreatic cancer invasion and metastases: a new paradigm for combination therapy in solid cancers. Cancer Res. 2007; 67:2187–96. [PubMed: 17332349]

18. Bailey JM, Singh PK, Hollingsworth MA. Cancer metastasis facilitated by developmental pathways: Sonic hedgehog, Notch, and bone morphogenic proteins. J Cell Biochem. 2007; 102:829–39. [PubMed: 17914743]

19. Yauch RL, Gould SE, Scales SJ, Tang T, Tian H, Ahn CP, et al. A paracrine requirement for hedgehog signalling in cancer. Nature. 2008; 455:406–10. [PubMed: 18754008]

20. Olive KP, Jacobetz MA, Davidson CJ, Gopinathan A, McIntyre D, Honess D, et al. Inhibition of hedgehog signaling enhances delivery of chemotherapy in a mouse model of pancreatic cancer. Science. 2009; 324:1457–61. [PubMed: 19460966]

21. O'Toole SA, Machalek DA, Shearer RF, Millar EK, Nair R, Schofield P, et al. Hedgehog overexpression is associated with stromal interactions and predicts for poor outcome in breast cancer. Cancer Res. 71:4002–14. [PubMed: 21632555]

22. Dierks C, Grbic J, Zirlik K, Beigi R, Englund NP, Guo GR, et al. Essential role of stromally induced hedgehog signaling in B-cell malignancies. Nat Med. 2007; 13:944–51. [PubMed: 17632527]

23. Sterling JA, Oyajobi BO, Grubbs B, Padalecki SS, Munoz SA, Gupta A, et al. The hedgehog signaling molecule Gli2 induces parathyroid hormone-related peptide expression and osteolysis in metastatic human breast cancer cells. Cancer Res. 2006; 66:7548–53. [PubMed: 16885353]

24. Johnson RW, Nguyen MP, Padalecki SS, Grubbs BG, Merkel AR, Oyajobi BO, et al. TGF-beta promotion of Gli2-induced expression of parathyroid hormone-related protein, an important osteolytic factor in bone metastasis, is independent of canonical Hedgehog signaling. Cancer Res. 2011; 71:822–31. [PubMed: 21189326]

25. Long F, Zhang XM, Karp S, Yang Y, McMahon AP. Genetic manipulation of hedgehog signaling in the endochondral skeleton reveals a direct role in the regulation of chondrocyte proliferation. Development. 2001; 128:5099–108. [PubMed: 11748145]

26. Long F, Chung UI, Ohba S, McMahon J, Kronenberg HM, McMahon AP. Ihh signaling is directly required for the osteoblast lineage in the endochondral skeleton. Development. 2004; 131:1309–18. [PubMed: 14973297]

27. St-Jacques B, Hammerschmidt M, McMahon AP. Indian hedgehog signaling regulates proliferation and differentiation of chondrocytes and is essential for bone formation. Genes Dev. 1999; 13:2072–86. [PubMed: 10465785]

28. Yuasa T, Kataoka H, Kinto N, Iwamoto M, Enomoto-Iwamoto M, Iemura S, et al. Sonic hedgehog is involved in osteoblast differentiation by cooperating with BMP-2. J Cell Physiol. 2002; 193:225–32. [PubMed: 12385000]

29. Kinto N, Iwamoto M, Enomoto-Iwamoto M, Noji S, Ohuchi H, Yoshioka H, et al. Fibroblasts expressing Sonic hedgehog induce osteoblast differentiation and ectopic bone formation. FEBS Lett. 1997; 404:319–23. [PubMed: 9119087]

30. Maeda Y, Nakamura E, Nguyen MT, Suva LJ, Swain FL, Razzaque MS, et al. Indian Hedgehog produced by postnatal chondrocytes is essential for maintaining a growth plate and trabecular bone. Proc Natl Acad Sci U S A. 2007; 104:6382–7. [PubMed: 17409191]

31. Kimura H, Ng JM, Curran T. Transient inhibition of the Hedgehog pathway in young mice causes permanent defects in bone structure. Cancer Cell. 2008; 13:249–60. [PubMed: 18328428]

32. Mak KK, Bi Y, Wan C, Chuang PT, Clemens T, Young M, et al. Hedgehog signaling in mature osteoblasts regulates bone formation and resorption by controlling PTHrP and RANKL expression. Dev Cell. 2008; 14:674–88. [PubMed: 18477451]

33. Ohba S, Kawaguchi H, Kugimiya F, Ogasawara T, Kawamura N, Saito T, et al. Patched1 haploinsufficiency increases adult bone mass and modulates Gli3 repressor activity. Dev Cell. 2008; 14:689–99. [PubMed: 18477452]

34. Weilbaecher KN, Guise TA, McCauley LK. Cancer to bone: a fatal attraction. Nat Rev Cancer. 2011; 11:411–25. [PubMed: 21593787]

35. Smith MC, Luker KE, Garbow JR, Prior JL, Jackson E, Piwnica-Worms D, et al. CXCR4 regulates growth of both primary and metastatic breast cancer. Cancer Res. 2004; 64:8604–12. [PubMed: 15574767]
36. Uluckan O, Becker SN, Deng H, Zou W, Prior JL, Piwnica-Worms D, et al. CD47 regulates bone mass and tumor metastasis to bone. Cancer Res. 2009; 69:3196–204. [PubMed: 19276363]
37. Guise TA, Yin JJ, Taylor SD, Kumagai Y, Dallas M, Boyce BF, et al. Evidence for a causal role of parathyroid hormone-related protein in the pathogenesis of human breast cancer-mediated osteolysis. J Clin Invest. 1996; 98:1544–9. [PubMed: 8833902]
38. Morgan EA, Schneider JG, Baroni TE, Uluckan O, Heller E, Hurchla MA, et al. Dissection of platelet and myeloid cell defects by conditional targeting of the beta3-integrin subunit. Faseb J. 2010; 24:1117–27. [PubMed: 19933310]
39. Mukherjee S, Frolova N, Sadlonova A, Novak Z, Steg A, Page GP, et al. Hedgehog signaling and response to cyclopamine differ in epithelial and stromal cells in benign breast and breast cancer. Cancer Biol Ther. 2006; 5:674–83. [PubMed: 16855373]
40. Buonamici S, Williams J, Morrissey M, Wang A, Guo R, Vattay A, et al. Interfering with resistance to smoothened antagonists by inhibition of the PI3K pathway in medulloblastoma. Sci Transl Med. 2010; 2:51ra70.
41. Yauch RL, Dijkgraaf GJ, Alicke B, Januario T, Ahn CP, Holcomb T, et al. Smoothened mutation confers resistance to a Hedgehog pathway inhibitor in medulloblastoma. Science. 2009; 326:572–4. [PubMed: 19726788]
42. Lauth M, Bergstrom A, Shimokawa T, Toftgard R. Inhibition of GLI-mediated transcription and tumor cell growth by small-molecule antagonists. Proc Natl Acad Sci U S A. 2007; 104:8455–60. [PubMed: 17494766]
43. Tian H, Callahan CA, DuPree KJ, Darbonne WC, Ahn CP, Scales SJ, et al. Hedgehog signaling is restricted to the stromal compartment during pancreatic carcinogenesis. Proc Natl Acad Sci U S A. 2009; 106:4254–9. [PubMed: 19246386]
44. Von Hoff D, Rudin C, LoRusso P, et al. Efficacy data of GDC-0449, a systemic hedgehog pathway antagonist, in a first-in-human, first-in-class phase I study with locally advanced, multifocal or metastatic basal cell carcinoma patients. Proc Am Assoc Cancer Res. 2008; 49:138.
45. Lorusso PM, Rudin CM, Reddy JC, Tibes R, Weiss GJ, Borad MJ, et al. Phase I Trial of Hedgehog Pathway Inhibitor Vismodegib (GDC-0449) in Patients with Refractory, Locally Advanced or Metastatic Solid Tumors. Clin Cancer Res. 2011; 17:2502–11. [PubMed: 21300762]
46. Brochure Is. GDC-0449. Genentech, Inc.; 2008.
47. Das S, Samant RS, Shevde LA. Hedgehog signaling induced by breast cancer cells promotes osteoclastogenesis and osteolysis. J Biol Chem. 2011; 286:9612–22. [PubMed: 21169638]
48. Uzawa T, Hori M, Ejiri S, Ozawa H. Comparison of the effects of intermittent and continuous administration of human parathyroid hormone(1-34) on rat bone. Bone. 1995; 16:477–84. [PubMed: 7605709]
49. Cao X, Geradts J, Dewhirst MW, Lo HW. Upregulation of VEGF-A and CD24 gene expression by the tGLI1 transcription factor contributes to the aggressive behavior of breast cancer cells. Oncogene. 2011
50. Chen W, Tang T, Eastham-Anderson J, Dunlap D, Alicke B, Nannini M, et al. Canonical hedgehog signaling augments tumor angiogenesis by induction of VEGF-A in stromal perivascular cells. Proc Natl Acad Sci U S A. 2011; 108:9589–94. [PubMed: 21597001]

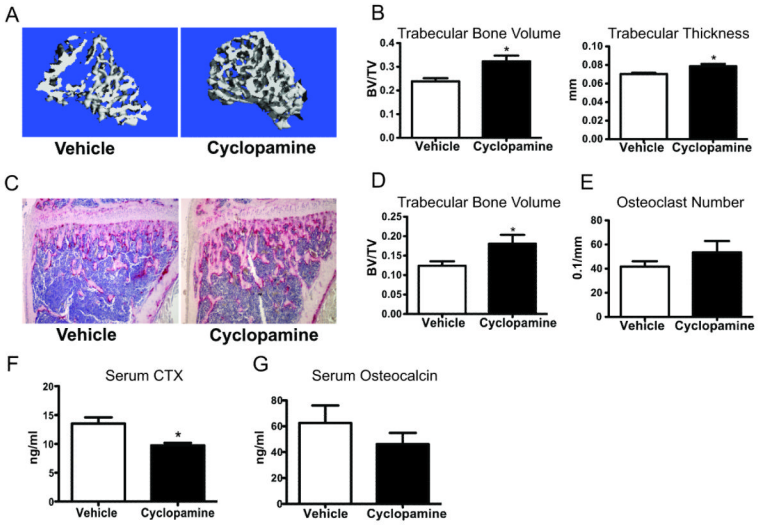

Figure 1. Cyclopamine increased bone mass and suppressed OC function in non-tumor bearing mice

8-week-old female C57Bl/6 mice treated with vehicle or cyclopamine for 14 days (n=7/group). A-B) μCT analysis for calculation of trabecular bone volume and trabecular thickness of tibiae C-E) Histomorphometry of tibiae stained for OC marker TRAP (red) to calculate: D) Trabecular bone volume and E) OC number (ns, p=0.28). F) Serum CTX and G) Serum osteocalcin (ns, p=0.37).

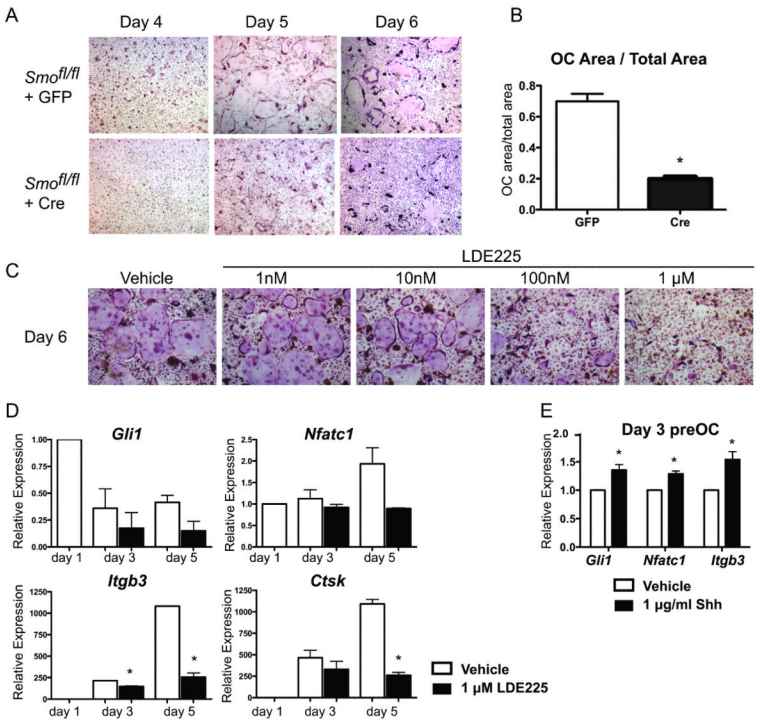

Figure 2. Disruption of Hedgehog signaling inhibited ex vivo osteoclastogenesis in a cell-autonomous manner

A) *Smo*$^{fl/fl}$ bone marrow derived macrophages were lentivirally infected with Cre-recombinase or GFP control to delete *Smoothened*, differentiated into OCs and stained with TRAP. B) Quantification of above OC area per total area on day 6. C) TRAP staining of OC differentiated in the presence of vehicle or LDE225 for 6 days. D) Treatment with 1μM LDE225 decreased *Gli1, Nfatc1, Itgb3*, and *Ctsk* transcripts by qRT-PCR on days 3 and 5 of OC differentiation. Data normalized to gene expression of day 1 vehicle treated macrophages. E) Day 3 preOC treated with 1μg/ml recombinant murine Shh for 24 hours had increased levels of *Gli1*, *Nfatc1*, and *Itgb3* by qRT-PCR.

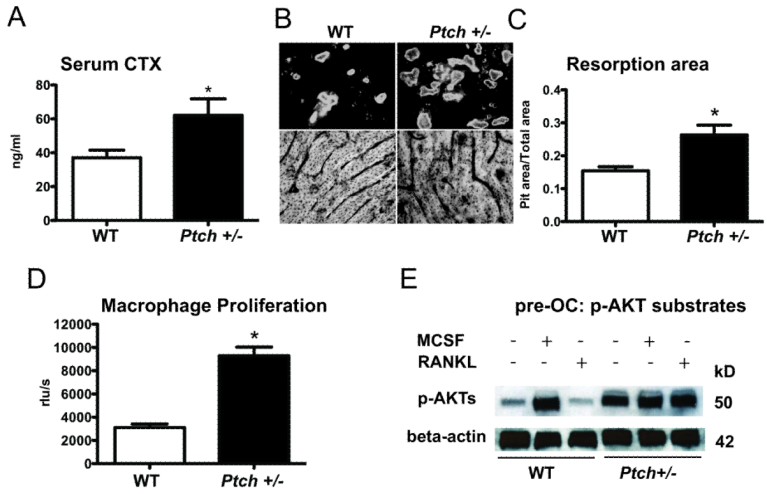

Figure 3. Enhanced Hedgehog signaling due to *Ptch1* heterozygosity increased OC function in a cell-autonomous manner

A) Serum CTX was increased in *Ptch1*+/− mice compared to WT littermates (n=7/group). B) Increased actin ring formation (top) and bone resorption lacunae (bottom) in *Ptch1*+/− OC differentiated on bovine bone slices for 6 days. C) Quantification of resorption lacunae area. D) Proliferation of *Ptch1*+/− and WT macrophages in response to 100 ng/mL MCSF by BrdU incorporation assay. E) Immunoblotting of p-AKT substrates and β-actin of *Ptch1*+/− and WT day 3 pre-OC starved for 1 hour and stimulated with 50 ng/mL MCSF or 50 ng/mL RANKL for 30 minutes.

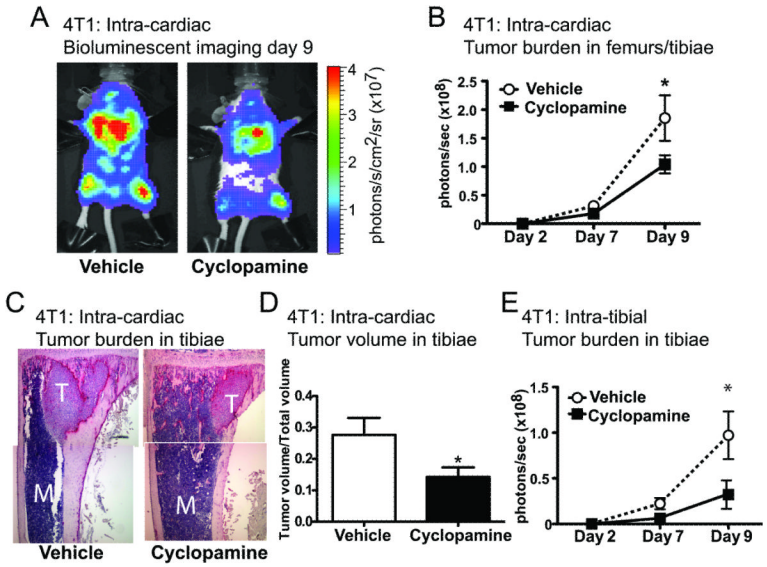

Figure 4. Hedgehog pathway inhibition with cyclopamine decreased bone metastases in a murine breast cancer model

A-D) Balb/c mice treated with vehicle (n=6) or cyclopamine (n=10) starting 1 day prior to left ventricular injection of 4T1. A-B) Tumor burden in femurs and tibiae as measured by in vivo bioluminescence (BLI). C-D) Histomorphometric analysis of tumor volume per total volume in tibiae by H&E on day 9. M=marrow; T=tumor. E) Cyclopamine treatment beginning on day -1 also decreased tumor burden following direct intra-tibial inoculation of 4T1 cells as measured by BLI.

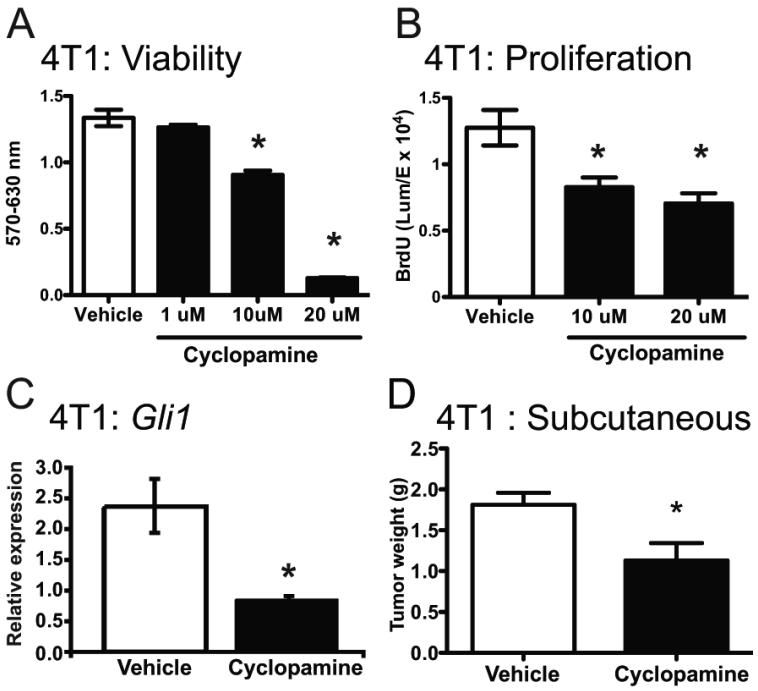

Figure 5. Smo antagonists exert direct cytotoxic effects on 4T1 breast cancer cells

4T1 cells treated for 24 hours with cyclopamine had decreased: A) viability as measured by MTT assay, B) proliferation as measured by BrdU incorporation, and C) expression of *Gli1* by qRT-PCR (10uM cyclopamine). D) Tumor weight on day 11 after subcutaneous injection of 4T1 cells into WT Balb/c mice after vehicle or cyclopamine (n=9/group) treatment starting on day -1.

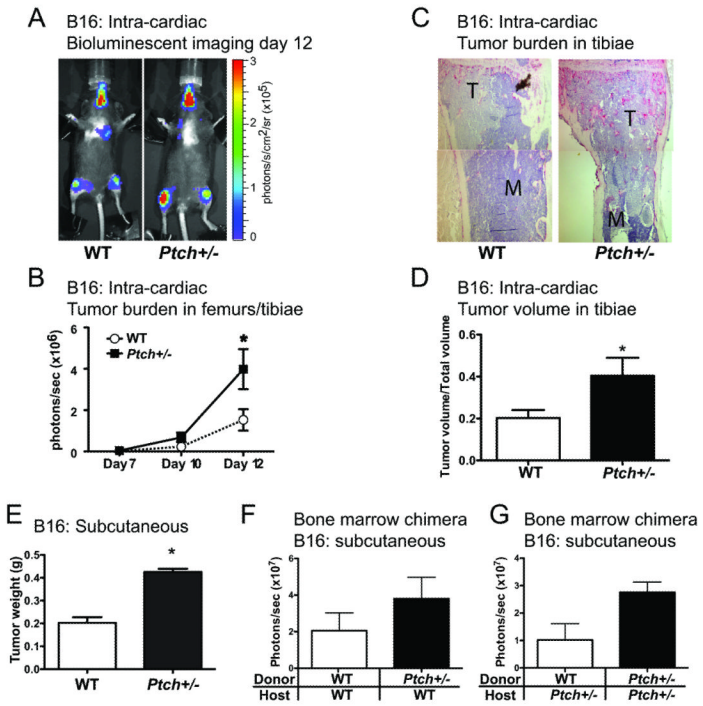

Figure 6. Enhanced Hh signaling due to Ptch1-heterozygosity indirectly enhanced tumor growth

A-D) Following intra-cardiac injection of B16 cells, tumor burden was increased in *Ptch1*+/− (n=6) mice as compared to WT littermates (n=5) by (A-B) BLI and (C-D) histomorphometric analysis of H&E stained tibiae on day 12. M=marrow; T=tumor. E) Tumor weight on day 11 after subcutaneous injection of B16 cells (WT, n=4; *Ptch1*+/−, n=5). F-G) B16 subcutaneous tumor burden by BLI on day 14 in WT and *Ptch1*+/− reciprocal bone marrow chimeras. F) Subcutaneous tumors of WT recipients of *Ptch1*+/− bone marrow (n=5) compared to recipients of WT bone marrow (n=5) (p=0.3009). G) *Ptch1*+/− recipients reconstituted with *Ptch1*+/− bone marrow (n=5) showed a trend toward increased tumor growth compared to those receiving WT bone marrow (n=4) (p=0.0760).

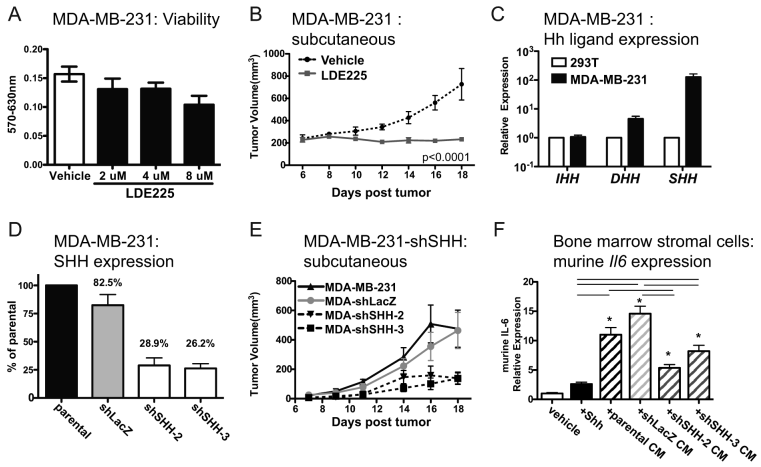

Figure 7. Tumor-derived Sonic hedgehog increased tumor growth through effects on the microenvironment

A) Viability of MDA-MB-231 human breast cancer cells is not decreased by LDE225 treatment in vitro as assayed by MTT. B) Subcutaneous growth of MDA-MB-231 in nude mice treated with LDE225 (n=6) or vehicle (n=4) starting day -2. C) MDA-MB-231 expression of Hh ligands relative to 293T cells by qRT-PCR. D) Expression of SHH by qRT-PCR following lentiviral-based shRNA knockdown of control LacZ (shLacZ) or SHH (2 independent shRNAs: shSHH-2 and shSHH-3) in MDA-MB-231 cells as compared to parental cells. E) Subcutaneous tumor growth of MDA-MB-231 parental (n=7), -shLacZ (n=8), -shSHH-2 (n=7) and –shSHH-3 (n=8) cells in nude mice. Repeated measures ANOVA: $p \leq 0.05$: parental vs. shSHH-2; parental vs. shSHH-3; shLacZ vs shSHH-3. shLacZ vs shSHH-2 p=0.0632. F) Murine bone marrow stromal cell (BMSC) expression of *Il6* by qRT-PCR following 72-hour culture with 1ug/ml Shh or conditioned media from MDA-MB-231 -parental, -shLacZ, -shSHH-2 or –shSHH-3 tumor cells. * indicates $p \leq 0.05$ vs. vehicle treated BMSC; lines (---) designate $p \leq 0.05$ between groups.